Spatially inhomogeneous inelastic electron tunneling in oxygen-ethylene complexes on Ag(110) resolved with a scanning tunneling microscope

J. R. Hahn[1,*] and W. Ho[2,†]

[1]*Department of Chemistry and Research, Institute of Physics and Chemistry, Chonbuk National University, Jeonju 561-756, Korea*

[2]*Department of Physics and Astronomy and Department of Chemistry, University of California, Irvine, California 92697-4575, USA*

(Received 3 September 2009; published 27 October 2009)

Inelastic electron-tunneling spectroscopy and microscopy with a scanning tunneling microscope revealed two vibrational modes of O_2 in single O_2-C_2H_4 complexes adsorbed on a Ag(110) surface at 13 K, showing both *increased* and *decreased ac* conductance. While both modes exhibit spatial variations in the intensity, the lower energy mode shows unexpected changes in the sign and lineshape of the peak. The observed spatial variations in the inelastic electron-tunneling signals may be induced by the broken symmetry of the O_2 due to the asymmetrically coadsorbed C_2H_4 and strong localization in the coupling between the vibrational motion and the electronic molecular orbitals.

DOI: 10.1103/PhysRevB.80.165428 PACS number(s): 68.35.Ja, 07.79.Cz, 34.50.Ez, 68.43.Pq

I. INTRODUCTION

The exceptional ability of the scanning tunneling microscope (STM) for the study of molecular adsorption at the single-molecule level has been greatly expanded with the demonstration of its ability to measure molecular vibrations through the detection of inelastic electron-tunneling (IET) processes.[1–9] STM-based IET spectroscopy (STM-IETS) is a very powerful tool for probing elementary excitations, such as vibrations, phonons, and plasmons, and for understanding the nature of chemical bonding and local chemical environment at the molecular level. STM-IETS detects the vibrational modes of a single molecule by measuring the total conductance change resulting from IET.[9–12] Observations of a wide range of vibrations and their changes in various chemical environments (e.g., in the presence of adsorbate-adsorbate interactions) should further broaden the usefulness of STM-IETS as an analytical technique. In addition to the vibrational spectra, high spatial resolution achieved in topographical imaging and vibrational microscopy provides insights into the nature of electron-vibration couplings of adsorbed molecules.

In the present study, we used STM-IETS to observe the spatial variations in vibrational intensity and lineshape of a single O_2 interacting with a nearby coadsorbed C_2H_4 on a Ag(110). Upon formation of single O_2-C_2H_4 complexes from isolated molecules, the tunneling conductance increases at the lower energy vibrational mode over the one O atom away from the C_2H_4. On the other O atom, however, the vibrational property is similar to that of the isolated O_2. We observe that the vibrational excitation process can be spatially localized and inhomogeneous in a single molecule. The O_2 on silver is a model system for studying interactions between adsorbed molecules because of its distinct states of O_2 adsorption at different temperatures. Between 40 and 150 K, O_2 is chemisorbed and the O-O bond is considerably weakened by electron transfer from the silver to the O_2 molecular orbitals.[13,14] Both O_2 and C_2H_4 are adsorbed parallel to the silver surface.[13–16]

II. EXPERIMENT

Experiments were carried out using a homemade, variable-temperature STM,[17] housed inside an ultrahigh vacuum chamber with a base pressure of 2×10^{-11} Torr. The Ag(110) sample was prepared by ion sputtering followed by annealing. The O_2 molecules were adsorbed on the sample at 45 K to ensure molecular chemisorption. The O_2 coverage was kept below 0.01 monolayer (ML). Following adsorption, the sample and the STM were cooled to 13 K. The C_2H_4 molecules are coadsorbed on the surface at 13 K (<0.01 ML).

III. RESULTS AND DISCUSSION

Figure 1(a) shows a STM topographical image of a physisorbed C_2H_4 and a chemisorbed O_2 molecule. The C_2H_4 appears as an oval-shaped protrusion elongated along the [001] direction on Ag(110) while the O_2 appears as an oval-shaped depression elongated along the $[1\bar{1}0]$ direction. The isolated C_2H_4 binds at the atop site, in agreement with theoretical calculations.[18] In addition, previous studies[16] revealed that (i) C_2H_4 adsorbs onto a Ag(110) surface via a weak bond, (ii) the adsorption is strongly promoted by the presence of adsorbed oxygen, and (iii) when coadsorbed with O atoms, C_2H_4 adsorbs selectively onto Ag atoms in which a positive charge has been induced by the O atoms. Theoretical calculations[18] predict that adsorption of C_2H_4 is 0.02 eV more favorable when the C=C axis is parallel to the $[1\bar{1}0]$ direction compared to the [001] direction [Fig. 1(b)]. For O_2, two predominant adsorption geometries have been identified,[9,19,20] one with the molecular axis aligned along the [001] direction of the substrate [O_2(001), Fig. 1(a)] and the other with the molecular axis aligned along the $[1\bar{1}0]$ direction [$O_2(1\bar{1}0)$, not shown]. The weak binding of C_2H_4 to Ag(110) enables the lateral manipulation of a C_2H_4 by maintaining an appropriate sample bias voltage and tunneling current at a substrate temperature of 13 K.[21] Specifically, the C_2H_4 was moved laterally by applying a positive sample voltage pulse of ~250 mV with feedback off after setting the tunneling gap over the molecule at a sample bias voltage of 70 mV and a tunneling current of 1 nA. By applying repeated voltage pulses, the C_2H_4 was moved to adjacent to

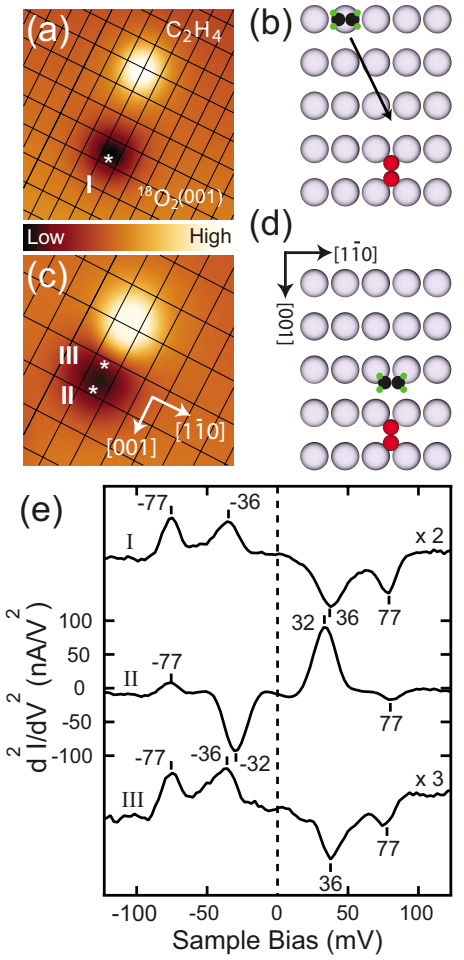

FIG. 1. (Color online) STM topographical images showing C_2H_4 and O_2(001) molecules adsorbed on Ag(110) and STM-IETS spectra recorded on the O_2(001). See the text for the notation. The images were obtained with a bare tip at 70 mV sample bias voltage and 1 nA tunneling current at 13 K. (a) An O_2(001) molecule and a C_2H_4 molecule separated by 14.5 Å. The scan area is 34×34 Å^2. (b) A schematic for the adsorption geometries of the molecules. The C_2H_4 is adsorbed on the on-top site and the O_2(001) is on the fourfold hollow site. The C_2H_4 was moved to the O_2(001) by applying sample bias voltage pulses (+250 mV) after positioning the tip over it, which led to the formation of an O_2(001)-C_2H_4 complex in (c). Arrow in (b) indicates the C_2H_4 movement. The scan area is 23×23 Å^2. (d) A schematic of the complex. In the diagrams, the smallest green, black, red (dark gray), and largest gray circles represent hydrogen, carbon, oxygen, and silver atoms, respectively. Grid lines in the images are drawn through the silver surface atoms, which can be resolved in the images obtained with a C_2H_4-terminated tip (Ref. 7) (e) STM-IETS spectra for O_2(001) at the positions marked by asterisks in images (a) and (c). The spectra displayed are averages of multiple scans from −125 to +125 mV and back with subtraction of the background spectrum taken over clean Ag(110).

the O_2(001), leading to the formation of a O_2(001)-C_2H_4 complex [Figs. 1(c) and 1(d)].

To investigate the change in the vibrational behavior of O_2(001) upon formation of the O_2(001)-C_2H_4 complex, we recorded vibrational spectra [Fig. 1(e)] with STM-IETS on positions I, II, and III over the O_2(001). The vibrational features were supported by oxygen isotope spectral shifts. At position I, the spectrum exhibited two dips at positive sample bias voltage (36 and 77 mV in curve I) and two corresponding peaks at negative bias. These two vibrational modes are assigned to the O-O stretch (77 meV) and antisymmetric O_2(001)-Ag stretch (36 meV), respectively.[9]

Comparing the spectra recorded at position I on the isolated O_2(001) and positions II and III on the O_2(001) in the complex, we observed two distinct changes associated with the formation of the complex. First, in curve II, we observed a large peak and a dip at positive sample bias voltage and a corresponding dip and peak at negative bias (curve II). The dip (peak) of the low-energy mode at positive (negative) sample bias in curve I is changed to a peak (dip) in curve II. The intensity of the 32 meV mode is approximately eight times higher than that at 77 meV. Second, the change in the lineshape causes an apparent shift in the low-energy mode (36 meV) in curve I to 32 meV in curve II while the energy of the higher energy mode (77 meV) remains unchanged. At position III, the vibrational energies of the two modes are the same as those of curve I and no changes in peak and dip structures are observed. We also note that the intensities of the higher energy mode in curves II and III are weaker than for isolated O_2 (curve I). These results show that the inelastic electron-tunneling cross section and lineshape vary with the position where the spectrum is obtained. To further characterize this effect on the spatial distribution, we recorded vibrational spectra at 11 positions over the complex and the isolated O_2(001) (Fig. 2).

Figure 2(c) shows the energy of the low-energy mode as a function of position above the O_2 for an isolated O_2(001) [Fig. 2(a)] and the O_2(001)-C_2H_4 complex [Fig. 2(b)]. The vibrational energies in this plot were determined from spectra recorded with the tip positioned at locations ***a***–***k*** along the [001] direction of the O_2 in each system. For the isolated O_2(001), the vibrational energy was ~36 meV at all positions except for the center (point ***f***), ***a***, and ***k***, where the intensity vanishes. For the O_2 in the complex, however, the vibrational energy was ~32 meV at positions ***b***–***e***, and ~36 meV at positions ***g***–***j*** [Fig. 2(d)]. It is interesting to note that the energy of the low-energy mode of the O_2 in the complex was the same as for the isolated O_2(001) (negative peak at 36 meV) on the C_2H_4 side of the complex (from ***g***–***j***) while the energy on the opposite side was 32 meV for the positive peak (from ***b***–***e***). In the case of the O-O stretch vibration, no differences in the spatial distribution of the vibrational energy and shape were observed compared to those of isolated O_2(001) [Fig. 2(d)].

The spatial distribution of the STM-IETS intensity (peak and dip) can also be probed by recording the topographic and vibrational images simultaneously at a fixed bias voltage, which is useful for understanding electron-vibrational coupling and the geometric structure of the complex. Figures 3(b) and 3(d) show vibrational images of an O_2(001)-C_2H_4 (32 meV) and an isolated O_2(001) (−36 meV), respectively. Simultaneous topographical [Figs. 3(a) and 3(c)] and vibrational imaging allows the spatial localization of the IET signal to be compared with the molecular topography. Cross-sectional cuts along the [001] direction [Figs. 3(e)–3(h)]

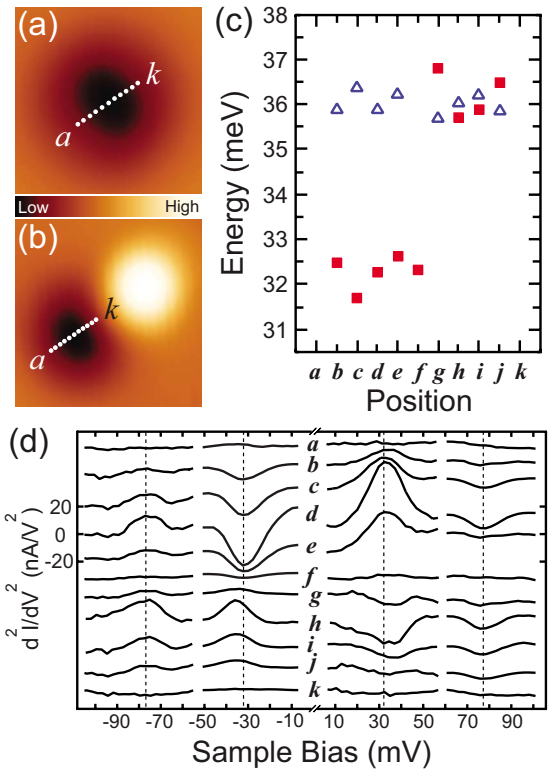

FIG. 2. (Color online) STM topographical images of (a) $O_2(001)$ and (b) the $O_2(001)$-C_2H_4 complex on Ag(110). (c) Open blue triangles and filled red squares indicate the positions of the low-energy vibration at positive bias for the $O_2(001)$ and $O_2(001)$-C_2H_4 complex, respectively. (d) Spatially resolved, background subtracted vibrational spectra of the $O_2(001)$-C_2H_4 complex on Ag(110). The spectra $\boldsymbol{a}$–$\boldsymbol{k}$ were obtained along the [001] direction and were fitted to determine the positions of the peaks or dips. The intensities of spectra $\boldsymbol{a}$–$\boldsymbol{f}$ obtained within ±55 mV were reduced by half in order to better show the high-energy vibration.

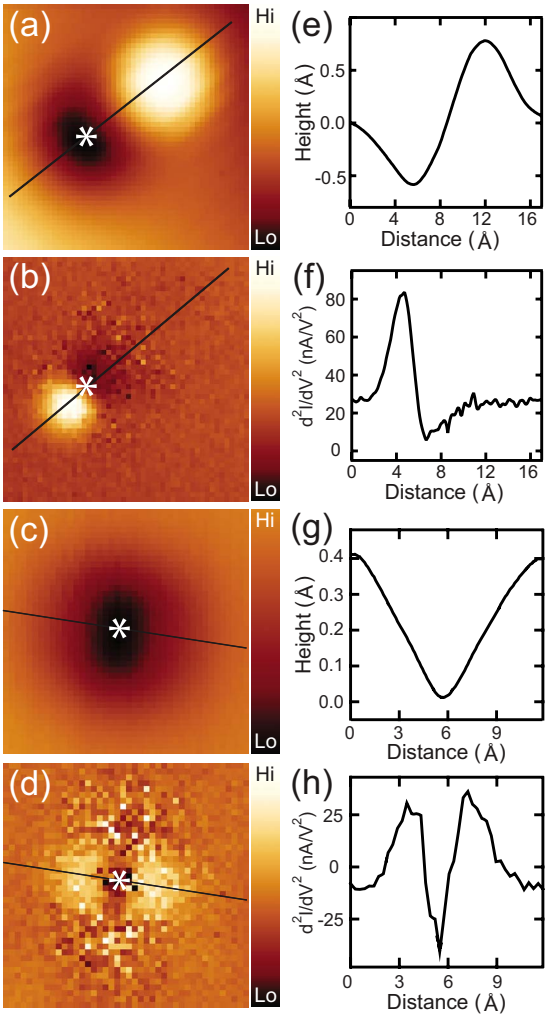

FIG. 3. (Color online) Comparison of the topographical images and the spatial distributions of STM-IETS intensities for the $O_2(001)$-C_2H_4 complex (32 meV) and the isolated $O_2(001)$ (−36 meV) vibrations on the Ag(110) surface. (a) Topographical image of the $O_2(001)$-C_2H_4 complex taken at 70 mV sample bias voltage and 1 nA tunneling current. (b) Vibrational image (32 meV) simultaneously recorded with the topographical image (a). The raw data, 15×15 Å^2 area, are shown at a resolution of 0.3 Å per pixel. (c) Topographical image of the isolated $O_2(001)$ taken at 70 mV sample bias voltage and 1 nA tunneling current. (d) Vibrational image (−36 meV) simultaneously recorded with the topographical image (c). The raw data, 12×12 Å^2 area, are shown at a resolution of 0.3 Å per pixel. (e), (f), (g), and (h) are cross-sectional cuts taken along the [001] direction (solid lines) in the images (a), (b), (c), and (d), respectively. The $O_2(001)$-C_2H_4 complex and the isolated $O_2(001)$ were studied on two different sample preparations when the surface crystallographic directions [001] and [1$\bar{1}$0] were not controlled.

reveal quantitative variations in the topographical and vibrational intensity. The highest and lowest intensities of the vibration in the $O_2(001)$-C_2H_4 complex occur when the tip is located ~1.5 Å away from the center (" * " in the image) of the $O_2(001)$ along the [001] direction. The positions of maximum and minimum vibrational intensity (peak at 32 meV and dip at 36 meV, respectively) are very close (within 0.1 Å) to those of the maxima (two peaks at −36 meV) of an isolated $O_2(001)$ [Fig. 3(d)]. Given that the vibrational intensity reflects in part the adsorption position and geometry of the molecule, these findings suggest that the geometric orientation of the $O_2(001)$ in the complex is not very different from that of the isolated $O_2(001)$. To form the complex [Fig. 1(c)], the C_2H_4 should be moved from the on-top silver atom to near the short bridge.

The observed spatial distribution of the vibrational intensity and lineshape of $O_2(001)$ indicates that the vibrational excitation process of the $O_2(001)$ in the complex is similar to that of the isolated $O_2(001)$ on one O atom but is different from that on the other O atom, i.e., the low-energy mode is observed at 32 meV and the tunneling conductance greatly increases (positive peak) at the vibrational excitation energy. Whether the tunneling conductance shows an increase or a decrease at the energy of vibrational excitation has important theoretical implications for understanding the mechanism of STM-IETS.[10,11,22] Two theoretical studies have predicted that both positive and negative contributions to the conductance are possible at the threshold energy of an inelastic process:[11,22] the inelastic contribution to the conductance induces a conductance increase whereas a decrease in conduc-

tance occurs at the same energy in the elastic channel. The latter are caused by the interference of electron states, which correspond to direct tunneling on the one hand and the excitation and reabsorption of virtual molecular vibrations on the other. For the case of O_2(001) on Ag(110), a resonant inelastic tunneling process occurs through the $1\pi_g$ orbital of O_2(001), which is an electronic orbital of the molecule overlapping with the Fermi level of the substrate. The onset of vibrational excitation leads to an overall decrease in the tunneling conductance due to the suppression of elastic tunneling.[9,22] Therefore, depending on which of the contributions (elastic or inelastic) prevails, various line shapes can appear in the spectra. The relative amounts of the two contributions depend on the coupling between the electronic states and vibrations, and changes in the adsorption features (geometry and charge states) of the molecule may modify this coupling. The present spatial distribution of conductance of O_2(001) indicates that the relative amounts of the two contributions depend on the position over the O_2(001) and is caused by the interaction with C_2H_4.

In the complex, the two O atoms are no longer equivalent since one O atom is closer to the C_2H_4 than the other and the symmetry of O_2 is reduced. The apparent frequency shift of 4 meV between 32 and 36 meV of this low-energy vibrational mode is due to a change in the lineshape, including the sign of the peak. The different spatial dependence of the elastic and inelastic contributions is shown to lead to a sign change in the IET signal from one side of the molecule to another due to the influence of the C_2H_4. The 32–36 meV mode is assigned to the antisymmetric O_2(001)-Ag stretch with each oxygen atom vibrating against the surface.[9] The O-O stretch energy at 77 meV is unchanged, indicating a negligible effect of the C_2H_4 on the O-O bond IET signal. The two molecules are too far apart to allow direct chemical bonding between them. The C_2H_4 indirectly interacts with the O_2(001) through the silver substrate and changes the spatial dependence of the IET cross section for the O_2(001)-Ag antisymmetric stretch. Although the O_2(001)-Ag stretch mode and the electronic states should be extended over the whole molecule, the coupling of the vibration to the molecular orbital is spatially inhomogeneous and highly localized, as well as the inelastic tunneling process.

IV. SUMMARY

In summary, we observed that the vibrational behavior of an isolated O_2 molecule adsorbed on Ag(110) is significantly changed when a C_2H_4 molecule is coadsorbed nearby. We found sudden changes in intensity and peak shape (sign) in the lower energy mode of O_2 when the STM-IETS is recorded along the O-O bond, whereas the higher energy mode only shows a variation in the intensity. This indicates that the vibrational excitation process, including the coupling of vibrational motion and the electronic molecular orbitals, can be spatially inhomogeneous and highly localized on a single molecule. These observations provide a special challenge in regard to the development of quantitative theories for, and fundamental understanding of, STM-IETS for coadsorbed, interacting molecules. Our results suggest that differences between molecular layer and single-molecule inelastic tunneling measurements could arise from the limited sampling of molecules in single-molecule experiments. The dependence of vibrational energy, intensity, and lineshape on the adsorption environment might explain the increase in the number of vibrational modes detected in molecular film measurements compared to STM-IETS measurements. Molecular films could potentially contain many molecular configurations and interactions. Understanding the conductance in molecular systems would require the identification of molecular modes that affect the conductance and knowing the differences between single-molecule and ensemble measurements.[23]

ACKNOWLEDGMENTS

This work was supported by the National Science Foundation under Grant No. DMR-0606520. In addition, J.R.H. thanks the KOSEF, funded by MOST (Grants No. R11-2007-012-02001-0 and No. R01-2007-000-20237-0).

*jrhahn@jbnu.ac.kr
†wilsonho@uci.edu

[1] B. C. Stipe, M. A. Rezaei, and W. Ho, Science **280**, 1732 (1998); W. Ho, J. Chem. Phys. **117**, 11033 (2002).
[2] T. Komeda, Prog. Surf. Sci. **78**, 41 (2005).
[3] H. Ueba, Surf. Rev. Lett. **10**, 771 (2003).
[4] J. I. Pascual, J. J. Jackiw, Z. Song, P. S. Weiss, H. Conrad, and H.-P. Rust, Phys. Rev. Lett. **86**, 1050 (2001); Surf. Sci. **502-503**, 1 (2002).
[5] M. Grobis, K. H. Khoo, R. Yamachika, Xinghua Lu, K. Nagaoka, Steven G. Louie, M. F. Crommie, H. Kato, and H. Shinohara, Phys. Rev. Lett. **94**, 136802 (2005).
[6] Y. Kim, T. Komeda, and M. Kawai, Phys. Rev. Lett. **89**, 126104 (2002).
[7] J. R. Hahn and W. Ho, Phys. Rev. Lett. **87**, 196102 (2001).
[8] L. Vitali, M. Burghard, P. Wahl, M. A. Schneider, and K. Kern, Phys. Rev. Lett. **96**, 086804 (2006).
[9] J. R. Hahn, H. J. Lee, and W. Ho, Phys. Rev. Lett. **85**, 1914 (2000).
[10] N. Mingo and K. Makoshi, Phys. Rev. Lett. **84**, 3694 (2000).
[11] N. Lorente and M. Persson, Phys. Rev. Lett. **85**, 2997 (2000); N. Lorente, M. Persson, L. J. Lauhon, and W. Ho, *ibid.* **86**, 2593 (2001).
[12] F. E. Olsson, M. Persson, N. Lorente, L. J. Lauhon, and W. Ho, J. Phys. Chem. B **106**, 8161 (2002).
[13] P. A. Gravil, D. M. Bird, and J. A. White, Phys. Rev. Lett. **77**, 3933 (1996).
[14] B. A. Sexton and R. J. Madix, Chem. Phys. Lett. **76**, 294 (1980).
[15] D. A. Outka, J. Stohr, W. Jark, P. Stevens, J. Solomon, and R. J. Madix, Phys. Rev. B **35**, 4119 (1987).

[16] C. Backx, C. P. M. de Groot, and P. Biloen, Appl. Surf. Sci. **6**, 256 (1980); C. Backx and C. P. M. de Groot, Surf. Sci. **115**, 382 (1982); C. Backx, C. P. M. de Groot, P. Biloen, and W. M. H. Sachtler, *ibid.* **128**, 81 (1983).

[17] The STM is a variation in the one described in B. C. Stipe, M. A. Rezaei, and W. Ho, Rev. Sci. Instrum. **70**, 137 (1999); L. J. Lauhon and W. Ho, *ibid.* **72**, 216 (2001); J. R. Hahn, Bull. Korean Chem. Soc. **26**, 1071 (2005).

[18] S. Gao, J. R. Hahn, and W. Ho, J. Chem. Phys. **119**, 6232 (2003).

[19] J. R. Hahn and W. Ho, J. Chem. Phys. **122**, 244704 (2005).

[20] J. R. Hahn and W. Ho, J. Chem. Phys. **123**, 214702 (2005).

[21] J. R. Hahn and W. Ho, J. Phys. Chem. B **109**, 20350 (2005).

[22] B. N. J. Persson and A. Baratoff, Phys. Rev. Lett. **59**, 339 (1987); B. N. J. Persson, Phys. Scr. **38**, 282 (1988).

[23] J. I. Pascual, J. Gómez-Herrero, D. Sánchez-Portal, and H. P. Rust, J. Chem. Phys. **117**, 9531 (2002).